1 INTRODUCTION **3**

2 BASICS OF ANTENNA THEORY: GAIN AND BEAM EFFICIENCIES **4**

2.1 Basics of Antenna Theory 4

2.2 Phenomenological Classification of Sidelobes and Definition of Terms 5

3 RELATIVE FEED-TO-FEED CAL VALUES FROM THE 21-CM LINE **6**

3.1 Phenomenological Rationale 6

3.2 Application and Results 6

4 RELATIVE FEED-TO-FEED GAINS AT 1420 MHz **8**

5 ABSOLUTE CAL VALUES FROM THE 21-CM LINE **10**

5.1 Theoretical Ratio of ALFA HI Antenna Temperature to HI Brightness Temperature 11

5.2 Observed Ratio of ALFA HI Antenna Temperature to HI Brightness Temperature . 12

6 ABSOLUTE GAIN FOR FEED 0 AT 1420 MHz **12**

6.1 Observational Determination 12

6.2 Theoretical Estimate 13

6.3 Tentative Adopted Value for On-Axis Gain at 1420 MHz 13

7 FREQUENCY DEPENDENCES **13**

7.1 Expected Frequency Dependence of the On-Axis gains 13

7.2 Frequency Dependence of Cal Values 14

7.3 Frequency Dependence of System Temperatures 16

7.4 Frequency Dependence of On-Axis Gains 16

8 TABLES OF FIDUCIAL VALUES AND SUMMARY **19**

8.1 Adopted Fiducial Values at 1420 MHz 19

8.2 Frequency Dependences 19

8.3 Three *ACTION ITEMS* 21

1. INTRODUCTION

In ATOMS 2000-02 and Heiles et al (2001) we developed a parameterization scheme to describe the main beam and its first sidelobe in all four Stokes parameters. In Heiles (2004, GALFA Technical Memo 2004-01) we applied the same model and technique to the Arecibo[1] ALFA beams for Stokes I and provided the parameters for ALFA's main beam and first sidelobes. That memo also provides technical details of the observations, which consist of 3 or 4 spider scans[2] on each beam during a few hours on 7 Nov 2004, and details of the reduction technique. We covered the band 1344-1444 MHz in 512 channels, which we binned to 32 channels each of width 3.125 MHz.

Here we extend the analysis and provide estimates for noise diode intensities ("cal values", T_{CAL}), on-axis gains ("gain", G_{max}), main beam efficiencies η_{MB}, and first sidelobe efficiencies η_{FS}. Here the term "efficiency" denotes the fraction of the total angle-integrated response that lies in the associated beam structure (§2). These are matters of absolute intensity calibration, which are very difficult to get accurately. For example, consider the gain, a seemingly simple quantity to determine: go to a point source of known flux, take $ON-OFF$, determine this deflection in terms of the known cal value, and you're done. The problem: many sources have "known" fluxes that aren't accurate and ditto for the cal values.

Here we consider several indications of gain and efficiency and use them all in a holistic approach to estimate these quantities. These indications include

1. Using the 21-cm line as an extended source to determine absolute cal values at 1420 MHz;
2. Using calibration sources to determine G_{max} at 1420 MHz;
3. Combining observational and theoretical estimates of gain and beam efficiencies to obtain fiducial values at 1420 MHz.
4. Using both observational and theoretical indications to determine the frequency dependences of cal values and gains.

We adopt a step-by-step procedure. The first step is the determination of relative cal values for all receivers at 1420 MHz using the HI line (§3), as first done by Giovanelli et al (2004). Next we use these relative cal values to obtain the relative gains for all 7 beams at 1420 MHz (§4); these show variations at the few percent level from beam to beam and these variations track the theoretically predicted ones. Next we use the LDS HI survey (Hartmann and Burton 1997) as an intensity standard, from which we derive absolute cal values (§5) and gains (§6). We derive frequency dependences in §7. Finally, §8 provides fiduciary values and summarizing remarks.

---

[1]The Arecibo Observatory is part of the National Astronomy and Ionosphere Center, which is operated by Cornell University under a cooperative agreement with the National Science Foundation

[2]Spider-scan calibration is the standard technique for Arecibo's single-pixel receivers.

Along our path we encounter certain questions that need either further investigation or monitoring in the future. We denote these as *ACTION ITEMS*. If we want ALFA to be a well-calibrated survey instrument, then it is important to put effort into these *ACTION ITEMS*.

2. BASICS OF ANTENNA THEORY: GAIN AND BEAM EFFICIENCIES

2.1. Basics of Antenna Theory

We follow Rohlfs and Wilson (2000) and define the directive gain G as the gain relative to an isotropic radiator for a single polarization. Conservation of energy requires that G satisfy the relationship

$$\int\int_{\text{whole sky}} G d\Omega = 4\pi \ . \tag{1}$$

The on-axis point-source directive gain is directly related to the effective area A_{eff} by

$$G_{\max} = \frac{4\pi A_{\text{eff}}}{\lambda^2} \ , \tag{2}$$

We now convert to practical units: $G_{max,KJy}$ is the on-axis gain in units of K Jy^{-1}, A_{eff} is in m^2, and k_B is Boltzmann's constant. This gives

$$G_{max,KJy} = 10^{-26} \frac{A_{\text{eff}}}{2k_B} \tag{3}$$

We relate the pure units to the practical ones by eliminating A_{eff}, which provides

$$G_{max} = \frac{3.47 \times 10^8}{\lambda^2_{\text{cm}}} G_{max,KJy} \ . \tag{4}$$

The normalized power pattern P_n has on-axis gain unity, so is just

$$P_n = \frac{G}{G_{max}} = 2.89 \times 10^{-9} \lambda^2_{\text{cm}} \frac{G}{G_{max,KJy}} \ , \tag{5}$$

so

$$\int\int_{\text{whole sky}} P_n d\Omega = 3.62 \times 10^{-8} \frac{\lambda^2_{\text{cm}}}{G_{max,KJy}} \ . \tag{6}$$

The "efficiency" of a portion of the telescope's beam is defined as the integral of the directive gain over that portion divided the integral over the whole sky. Thus, using units of arcmin^2 for Ω and cm for λ,

$$\eta_{\rm portion} = 2.34 \frac{G_{max,KJy}}{\lambda^2_{\rm cm}} \int\int_{\rm portion} P_n d\Omega_{\rm arcmin^2} \ . \tag{7}$$

Normally one speaks of the main beam efficiency, but we can also use the same terminology for any set of the sidelobes.

2.2. Phenomenological Classification of Sidelobes and Definition of Terms

We will need to distinguish the efficiency of the combination of the main beam and near-in sidelobes from that of the far-out sidelobes. Thus we define the "local" region, which consists of the main beam (efficiency η_{MB}) and near-in sidelobes (efficiency η_{nearin}). The efficiency of this portion of the beam is

$$\eta_{local} = \eta_{MB} + \eta_{nearin} \ . \tag{8}$$

We assume that η_{local} is the same for each ALFA feed. This is tantamount to assuming that any power removed from the main beam by the off-axis aberrations of feeds 1-6 appears in near-in sidelobes, not far-out ones; this assumption makes sense because the far-out sidelobes come from scattering off of physical structures, and because the rays for all feeds are nearly parallel they should all suffer comparable scattering.

There are also far-out sidelobes. As with the near-in sidelobes, we assume that the total efficiency in the far-out sidelobes is the same for each ALFA feed. Far-out sidelobes are produced by scattering off of physical structures in the beam. This scattering should be comparable for all feeds because their ray paths are nearly coincident and parallel.

Finally, some of the telescope's response is lost to ohmic dissipation, and we can express this as an efficiency. With this division of the telescope response, we have

$$\eta_{local} + \eta_{farout} + \eta_{ohmic} = 1 \ . \tag{9}$$

3. RELATIVE FEED-TO-FEED CAL VALUES FROM THE 21-CM LINE

3.1. Phenomenological Rationale

If we observe an area that is larger than the local region defined above, then typically each ALFA beam looks over the full extent of the region during the mapping process; different beams cover different positions, but only on the scale of arcmin. If the HI line varies smoothly over the region, or if the angular structure is sufficiently random, then we can rather accurately characterize the whole area by a single HI profile, the *mean HI profile* for the region. For each ALFA beam, we take the average profile over the whole map; each of the 7 ALFA profiles should be close to the mean HI profile.

However, the 7 ALFA HI profile intensities will differ if the cal values are not quite correct. We derive correction factors by forcing the 7 intensities to be identical, keeping the mean of the values equal to the originally-assumed ones, which come from the ALFA web page. Specifically, we use the values from the Oct 4, 2004 web page `alfa.naic.edu/performance/spectral-scans/Tcal/wide/` (Deshpande 2004). We are not the first to implement this technique; Giovanelli et al (2004: hereafter G04) did the same, using a large number of independent measurements spread over the sky, and we compare our results with theirs.

3.2. Application and Results

We mapped a 150 square degree region centered on $(\alpha, \delta) = (6^h45^m, 30^\circ)$ during about 16 hours in Oct-Nov 2004. We assume that our region is larger than the local region defined above and derive revised cal values using the above technique.

Table 1 shows the results. Columns 1 and 2 tell the feed/polarization. Column 3 gives $T_{CAL,WEB}$, the original cal value we obtained from the web page; column 4 gives $T_{CAL,GALFA}$, our revised values from the HI comparison, and column 5 gives the percent difference. If we assume the relative values of $T_{CAL,GALFA}$ to be correct, then column 5 illustrates the precision to which the web cal values are measured. If we exclude feed 5 from the comparison, the precision is usually better than 1%. We conclude that the relative values from one receiver to another, given on the web page are very good. The ALFA commissioning staff, the astronomers, and the engineers are to be congratulated on this good agreement! In fact, the good agreement at 1420 MHz is remarkable, considering that the cal values vary with frequency at the 10% level (section 7.2).

However, there remains the wildly discrepant feed 5. If we assume that the polarizations for feed 5 were inadvertently interchanged, then feed 5 would be as good as the other feeds. However, the individuals involved in these calibrations do not believe this is the case. These include Josh Goldston, who copied our cal values from the web page; Riccardo Giovanelli, the EGALFA group leader; and Phil Perillat, who provided important software and recently double-checked the cabling.

Column 6 gives $T_{CAL,EALFA}$, the HI-determined values from the EALFA group reported in R04, and column 7 gives the percent difference between $T_{CAL,GALFA}$ and $T_{CAL,EALFA}$. The variations from one feed/polarization entity to another should be identical because both groups used the same technique, so the values in column 7 should be zero (apart from statistical fluctuations). Unfortunately, however, the agreement is more than merely disappointing, given the fact that both groups claim precision at the 1% level: percentage differences for 6 entities, almost half, exceed 4%. Two of these are feed 5, which would be much ameliorated if the polarizations were inadvertently interchanged on GALSPECT with respect to the WAPPS. Similarly, if the two polarization cables for feed 2 to the WAPPS were interchanged, this would ameliorate the large percentage differences in the last column of Table 1. But, as mentioned above, the individuals involved do not believe this possibility.

The problem might be time variation of the cal values. The EGALFA group's calibrations extended over more than a month and Giovanelli has found some indication for time variability at the few percent level, particularly for feeds 5 and 6.

TABLE 1. CAL VALUES FOR ALL FEED/POLS

FEED	POL	$T_{CAL,WEB}$	$T_{CAL,GALFA}$	% DIFF GALFA–WEB	$T_{CAL,EALFA}$	% DIFF EALFA–GALFA
0	0	10.88	11.03	1.4	11.27	2.2
0	1	10.31	10.36	0.5	10.77	4.0
1	0	10.15	10.07	–0.8	10.03	–0.4
1	1	10.86	10.83	–0.3	10.67	–1.4
2	0	11.59	11.51	–0.7	10.65	–7.4
2	1	10.39	10.43	0.4	11.22	7.5
3	0	10.97	10.88	–0.8	10.53	–3.2
3	1	9.86	9.80	–0.6	10.36	5.8
4	0	10.47	10.35	–1.1	10.33	–0.2
4	1	10.56	10.68	1.1	10.34	–3.2
5	0	10.24	9.88	–3.5	10.50	6.2
5	1	9.70	10.31	6.3	9.19	–10.9
6	0	10.77	10.66	–1.0	10.93	2.5
6	1	10.68	10.56	–1.1	10.56	0.0
				RMS=2.1		RMS=5.2

Table 2 provides polarization-averaged values. The $T_{CAL,GALFA}$ and $T_{CAL,EALFA}$ values agree *much* better than in Table 1: the dispersion of the differences in column 6 is 1.9%, smaller by a factor of 2.7 than in Table 1 and not much higher than the 1.4% expected if the intrinsic dispersion of the

values is 1%, which is the precision claimed by each group. It is comforting that the polarization averages are so good. Their much better agreement again suggests a problem with polarization reversal, but we repeat that the individuals involved deny this possibility. We are left with this mystery.

TABLE 2. CAL VALUES FOR ALL FEEDS, POL-AVERAGED

FEED	$T_{CAL,WEB}$	$T_{CAL,GALFA}$	% DIFF GALFA–WEB	$T_{CAL,EALFA}$	% DIFF EALFA–GALFA
0	10.60	10.69	0.8	11.02	3.1
1	10.50	10.45	–0.5	10.35	–0.9
2	10.99	10.97	–0.2	10.94	–0.3
3	10.41	10.34	–0.7	10.45	1.1
4	10.52	10.51	–0.1	10.33	–1.7
5	9.97	10.10	1.3	9.84	–2.5
6	10.72	10.61	–1.0	10.74	1.3
			RMS=0.9		RMS=1.9

We will proceed using our values, $T_{CAL,GALFA}$. The relative values from one feed/polarization to another should be quite good, but all values are subject to a single, overall uncertain scale factor. We will deal with this scale factor later in §5.

4. RELATIVE FEED-TO-FEED GAINS AT 1420 MHz

Our spider-scan patterns supply the point source gains, which are equal to the source deflection in Kelvins (determined relative to the cal values) divided by the source flux. We observed two sources, B0540+187 and B0758+143. They yield gains that differ by 9.3%. This illustrates the lack of precision with which supposedly good calibrator fluxes are known.

For feed-to-feed comparisons we want to average together all data from the 3 or 4 observations for each feed; each feed observed both sources. We force the gains from the two sources to be identical by adjusting their two fluxes: we multiplied the official flux of B0540+187 by $\sqrt{1.093}$ and divided the other by the same factor.

Figure 1 shows the derived G_{max} versus feed/polarization (top panel) and zenith angle (bottom panel). In the top panel, circles show individual measurements of a single feed/polarization entity, and crosses show the average of all measurements in both polarizations for each feed. There are clear systematic differences from one feed to another, while the two polarizations for each feed agree quite well. Any dependence on zenith angle is obliterated by the feed-to-feed differences.

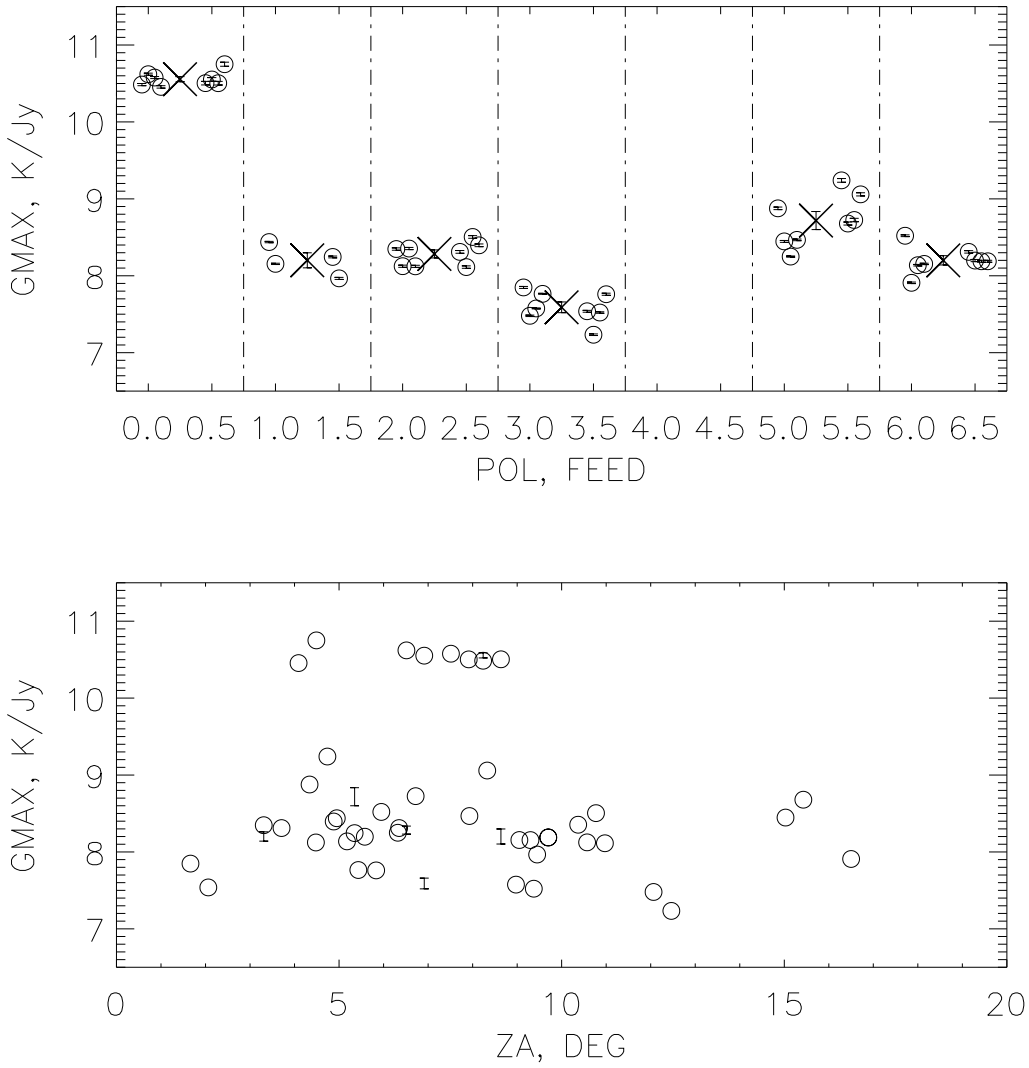

Fig. 1.— G_{max} from source deflections versus feed/polarization (top panel) and zenith angle (bottom panel). In the to panel, circles show individual measurements of a single feed/polarization entity, and crosses show the average of all measurements in both polarizations for each feed.

We compare the feed-to-feed differencees with theory by listing the polarization-averaged observed gains and the theoretical gains from Cortés-Medellin (2002; hereafter CM02). One caveat is that the theoretical gains are presented in graphical form with a fairly compressed scale; we read them by hand using a ruler, which introduces some error.

Table 3 shows both the observed and theoretical gains for each feed. Here our focus is on

relative gains, not absolute ones. Accordingly, we normalize them to identical scales by dividing each set by its mean and then by the theoretical gain for feed 0, making feed 0's gain equal to unity. In Table 3, we calculated GALFA GAIN from $T_{CAL,GALFA}$; WEB from the original web cal values; and EALFA GAIN from $T_{CAL,EALFA}$.

TABLE 3. RELATIVE GAINS, THEORY AND OBSERVED

FEED	THY GAIN	GALFA GAIN	% DIFF GALFA-THY	WEB GAIN	% DIFF WEB-THY	EALFA GAIN	% DIFF EALFA-THY
0	1.000	0.997	-0.3	0.988	-1.2	1.027	2.7
1	0.767	0.778	1.4	0.783	2.0	0.770	0.4
2	0.802	0.790	-1.5	0.791	-1.4	0.786	-2.0
3	0.740	0.725	-2.1	0.730	-1.4	0.732	-1.1
4	0.740	0.734	-0.8	0.734	-0.8	0.721	-2.6
5	0.802	0.817	1.9	0.806	0.5	0.795	-0.8
6	0.767	0.777	1.3	0.786	2.4	0.787	2.5
			RMS=1.6		RMS=1.6		RMS=2.1

The agreement is excellent for GALFA and WEB cal values, and is very good for the EALFA ones: the dispersions are 1.6%, 1.6%, and 2.1%, respectively. Given our ruler-reading uncertainties for the theoretical gains, the differences are not significant, especially for the first two columns. And consider columns 4 and 6 in detail: the percentage differences track each other accurately (meaning that, in fact, the two sets of cal values are nearly identical, as is clear from Table 1).

ACTION ITEM: We believe that the HI technique is valid and it has the advantage of providing accurate empirically-determined cal values that can be easily monitored over time for changes. For now, we adopt those cal values, i.e. the values of $T_{CAL,GALFA}$. In the future we will rederive these cal values for each area we map so that we can both maintain a historical record of changes and also gradually add to the precision with which the relative cal values are known at 1420 MHz. Giovanelli's discovery of time variability of the cal values underscores the importance of such monitoring.

5. ABSOLUTE CAL VALUES FROM THE 21-CM LINE

The introduction discussed the difficulties in obtaining accurate values for the intensity-related quantities. These include the cal values T_{CAL}, the on-axis gains G_{max}, the main beam efficiencies η_{MB}, and the first sidelobe efficiencies η_{FS}. It is one thing to derive accurate *relative* values, as we did above, but quite another to obtain the *absolute* values because they depend on knowing source fluxes and cal values.

Above in §2 we discussed the concept of beam efficiency and defined the efficiencies associated with the local region, the far-out sidelobes, and ohmic losses, and in §3.1 we argued that all ALFA beams should have nearly identical responses for the local region, and also for the far-out sidelobes.

We therefore assume that all HI power that looks like the true profile in our region comes from the combination of main beam and near-in sidelobes. We assume that the HI picked up by far-out sidelobes is distributed widely in apparent velocity and does not noticeably contribute to observed profile. We use the LDS HI survey to obtain the true profile, and forcing the intensities to be identical allows us to determine our absolute cal values.

5.1. Theoretical Ratio of ALFA HI Antenna Temperature to HI Brightness Temperature

Our approach is to obtain η_{local} in equation 9 from theoretical estimates of η_{farout} and η_{ohmic}. For far-out sidelobes, CM02 provides an "assumed value" for "Scattering and Blockage" (his Table 6.1). We assume that this diverts power into the far-out sidelobes, so η_{farout} is equal to his number, i.e.

$$\eta_{farout} = 0.062 \ . \tag{10}$$

For ohmic losses, CM02 estimates $\eta_{ohmic} = 0.23\%$ (Table 6.1, "Insertion losses"). He also estimates the fraction of power lost to secondary feed spillover at 1420 MHz to be 3.6% (Figure 4.1); this is equivalent to ohmic loss because the power scatters around the Gregorian dome until it dissipates and adds to system temperature, so it doesn't go to the sky. For the total ohmic loss we adopt the sum of these two,

$$\eta_{ohmic} = 0.038 \ . \tag{11}$$

The upshot is that we expect

$$\eta_{local} = 1 - \eta_{farout} - \eta_{ohmic} = 0.90 \ . \tag{12}$$

In words, this means that we expect the antenna temperature for any ALFA feed to be 0.90 times the brightness temperature of HI. The caveat is that the HI should vary slowly with angle over the local region of the ALFA beams, which is probably no more than a few degrees in size. With this caveat, we have

$$T_B(HI) = \frac{T_A(ALFA)}{\eta_{local}} \ . \tag{13}$$

5.2. Observed Ratio of ALFA HI Antenna Temperature to HI Brightness Temperature

We use the LDS HI survey as a standard of HI brightness temperature. The LDS ultimately derives its intensity scale from IAU standard regions S7 and S8, for which the definitive discussion is Kalberla, Mebold, & Reif (1982). Their discussion shows that variations of up to 4% exist from region to region, and observatory to observatory. Thus, we regard the absolute calibration of LDS as uncertain at the few percent level.

The LDS survey shows that the HI structure satisfies the above caveat regarding angular smoothness. We averaged the LDS HI line intensity over our observed region. We regard this as the true brightness temperature of the region. We compared it to the average of our own ALFA data over the region. To achieve agreement, we must multiply our intensities by 1.075. In contrast, if our cal values were perfectly correct, then equation 12 predicts we would have to multiply by 1.10 instead of 1.075. We note, parenthetically, that these numbers only differ 2.5%!

We therefore find, from this technique, that our cal values are 2.5% high. This number should be accurate to within a few percent (meaning it is not very precise, i.e., it's perhaps $2.5\% \pm 3\%$). We use this to convert our original GALFA cal values, column 4 in Table 1, to obtain the final adopted fiducial cal values in columns 2 and 3 of Table 4. The correction is so small it's hardly worth doing, but the specification of this factor for this epoch is an entry in what we hope will become a historical record of cal values and their behavior with time and ALFA position angle.

6. ABSOLUTE GAIN FOR FEED 0 AT 1420 MHz

6.1. Observational Determination

Given the fiducial cal values determined above in §5.2 and the fluxes of the two sources we obtain direct measurements of the on-axis gain for feed 0. As noted above, the two sources give gains that differ by 9.3% and we adjusted their fluxes to give the same answer. The result is that, for feed 0, we obtain

$$G_{max} = 10.53 \text{ K Jy}^{-1} \ . \tag{14}$$

Action Item: The above value should be refined by observing primary calibration sources whose fluxes are *truly* accurately known.

6.2. Theoretical Estimate

CM02 estimates the theoretical gain in Figures 6.4 and 7.1. We estimated its value visually using a ruler and obtain 11.0 K Jy^{-1} at 1375 MHz. Below we estimate that the gain $\propto f^{-0.23}$, so this translates to 10.9 K Jy^{-1} at 1420 MHz.

6.3. Tentative Adopted Value for On-Axis Gain at 1420 MHz

We adopt the average of the observational and theoretical estimates above. Note our *ACTION ITEM* that the observational estimate could easily be improved by observing primary calibrators with accurately known fluxes. Our tentative adopted value is

$$G_{max} = 10.72 \text{ K Jy}^{-1} \ . \tag{15}$$

7. FREQUENCY DEPENDENCES

In this section we consider the frequency dependence of the cal values, on-axis gains, and beam/first-sidelobe efficiencies.

7.1. Expected Frequency Dependence of the On-Axis gains

First, we consider the expected frequency dependence of the on-axis gain G_{max}. In GALFA Tech Memo 2004-01, we found the ALFA HPBWs to vary less rapidly with frequency than they would if the diameter of the illuminated area of the primary reflector were constant. Rather, our results were consistent with the illuminated area A varying as

$$A \propto \left(\frac{f}{1420}\right)^{-0.48} \ . \tag{16}$$

There is an additional frequency dependence, which is the increase in feed spillover efficiency with frequency shown in CM02, Figure 4.1. This power is scattered out of the main beam, so it reduces the gain. This contribution goes as

$$\eta_{spillover} \propto \left(\frac{f}{1420}\right)^{0.25} \ . \tag{17}$$

Combining these, we expect the on-axis gain G to vary as

$$G_{max} \propto \left(\frac{f}{1420}\right)^{-0.23} \quad . \tag{18}$$

7.2. Frequency Dependence of Cal Values

We can use equation 18 to derive the cal values by comparing frequency dependences of the the cal and source deflections. We note that while the absolute flux densities of sources are not necessarily known accurately, the frequency dependences are usually known quite well. Figure 2 shows the frequency dependence of the cal values for each feed/polarization entity, determined according to the above assumption. Specifically, the plotted cal value $T_{CAL}(f)$ is

$$T_{CAL}(f) = \left(\frac{f}{1420}\right)^{-0.23} \left(\frac{G'_{max}(1420)}{G'_{max}(f)}\right) T_{CAL}(1420) \ , \tag{19a}$$

where $G'_{max}(f)$ is the apparent on-axis gain in K Jy^{-1} calculated using the cal value at 1420 MHz, i.e.

$$G'_{max}(f) = \frac{T_{src,CAL=1420}(f)}{S_{src}(f)} \ , \tag{19b}$$

where $T_{src,CAL=1420}(f)$ is the source deflection at frequency f in Kelvins calculated using the cal value at 1420 MHz, which is itself denoted as $T_{CAL}(1420)$.

The solid lines in Figure 2 are the results for 3 or 4 independent observations and the dashed line is a 7-degree polynomial fit to the average of the observations, displaced downwards by 0.5 K for clarity. Results for feed 4 are lousy because the levels were incorrectly set.

The cal values exhibit irregular variations at the 10% level. These variations have been seen previously (Deshpande 2004). Some of these variations have narrow frequency structure, narrower even than our bandwidth of 3.125 MHz. The 7-degree polynomial fit does not perfectly reproduce the cal values; there are occasional bumps and wiggles on smaller frequency scales. One could fix this by using higher-order polynomials. However, in both spectral line and continuum observations one usually averages the cal values over bandwidths that exceed our resolution of 3.125 MHz, meaning that there isn't much reason to reproduce the fine-scale wiggles.

The rapid frequency variation is completely unexpected. In our experience, radioastronomical cal values generally do not have such rapid variations with frequency. We suspect that the variations occur because a single cal is split 14 ways to provide correlated noise to the different receivers. Mismatches in the splitters, or some of the inserted power being radiated out of the feeds and being picked up by other feeds, could produce mutual interference and lead to such frequency structure.

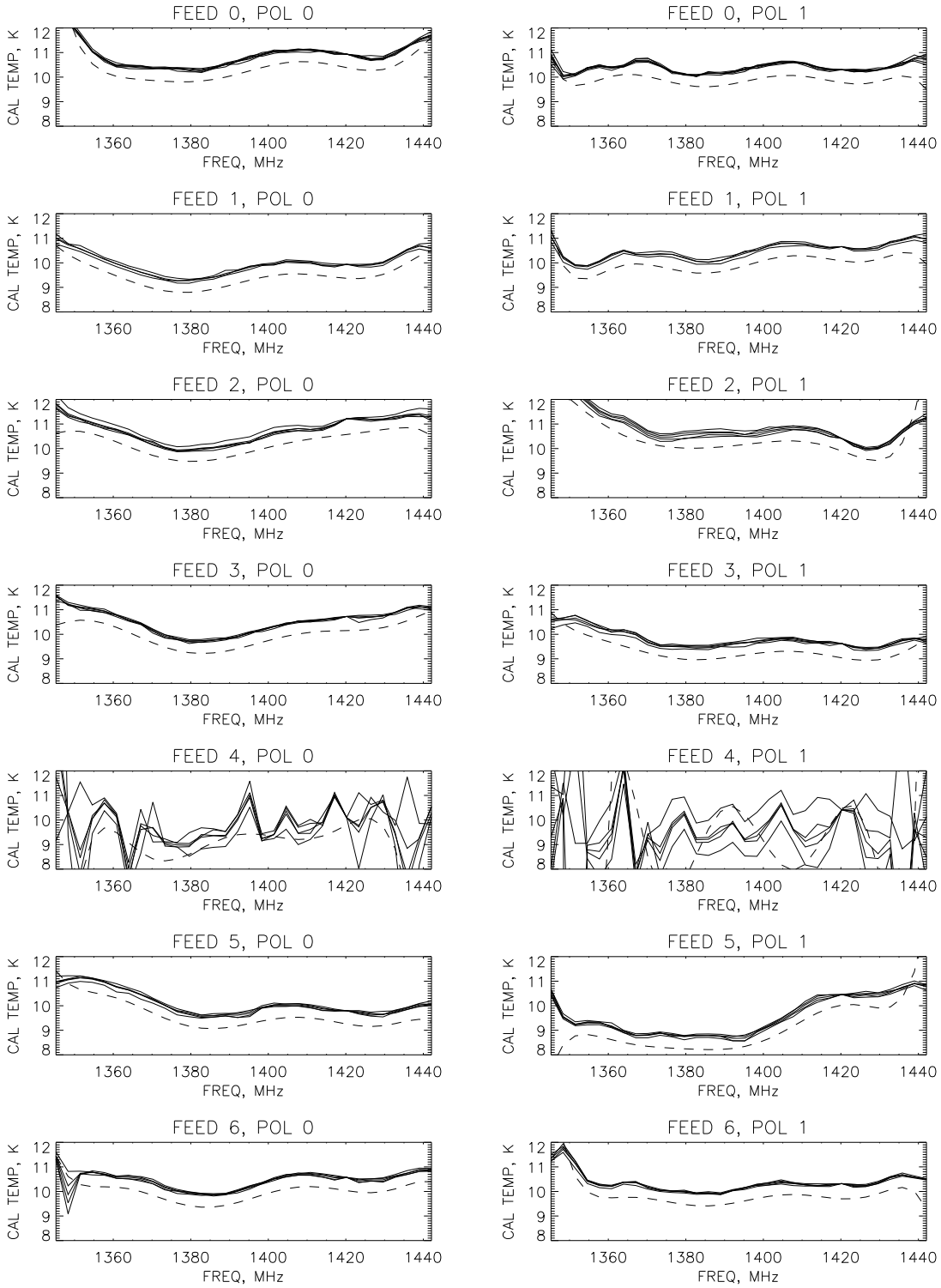

Fig. 2.— Cal values versus frequency for each feed/polarization entity. Each solid line represents an independent observation and the dashed line is a 7-degree polynomial fit to their average. The dashed line is displaced down by 0.5 K for clarity. Feed 4 values are (obviously) no good.

This is a problem because either process would probably depend sensitively on the exact way in which reflections interact with each other. The frequency variations, in turn, might well change with time and/or ALFA rotation angle.

We recall that Giovanelli discovered time variations in cal values (§3). Moreover, if one compares the frequency dependences in our Figure 2 with those of Desh on the ALFA web page, one sees differences. We speculate that these differences and variations are related to the rapid frequency structure and are indicative of this interference process.

ACTION ITEM: We suggest that the dependences of cal values on frequency and ALFA rotation angle and time be determined and monitored regularly.

7.3. Frequency Dependence of System Temperatures

Figure 3 shows the frequency dependence of the system temperature for each feed/polarization entity, determined using the polynomial fits to the cal values shown in Figure 2. As in Figure 2, each solid line represents an independent observation. The observations show systematic differences from one observation to another. These observations occurred at different zenith angles, which is probably responsible for some of the variation.

The system temperatures show two types of variation with frequency. One is the gradual increase towards lower frequency. This agrees well, semiquantitatively speaking, with CM02, who predicted an increase of roughly 3.3 K per 100 MHz (his Figure 6.4.3). There also exist bumps and wiggles on smaller frequency scales. Some of the bumps are not intrinsic to the receivers; for example, the excess system temperature at 1420 MHz is the HI line.

7.4. Frequency Dependence of On-Axis Gains

Figure 4 shows the frequency dependence of the on-axis gain for each feed/polarization entity, determined using the polynomial fits to the cal values shown in Figure 2. As in Figure 2, each solid line represents an independent observation. The observations show systematic differences from one to another. These observations occurred at different zenith angles, which is probably responsible for some of the variation.

The gains show two types of variation with frequency. One is the gradual increase towards lower frequency, which matches equation 18. For a few feed/polarization entities, e.g. feed 0, pol 1, there also exist bumps and wiggles on smaller frequency scales; these occur because the polynomial fits do not perfectly reproduce the cal values.

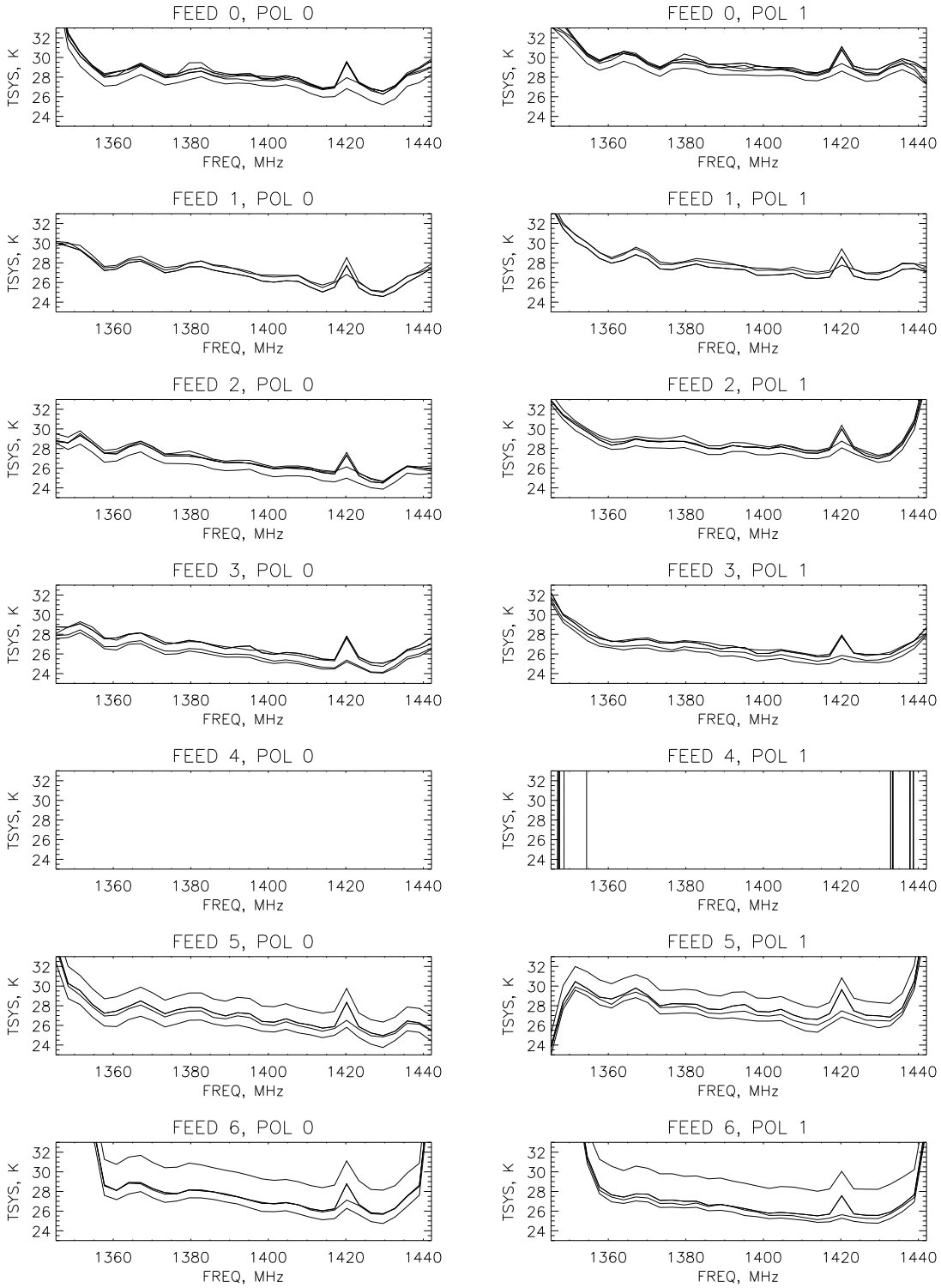

Fig. 3.— System temperatures versus frequency for each feed/polarization entity derived from the cal values in Figure 2. Each solid line represents an independent observation. Feed 4 values are no good.

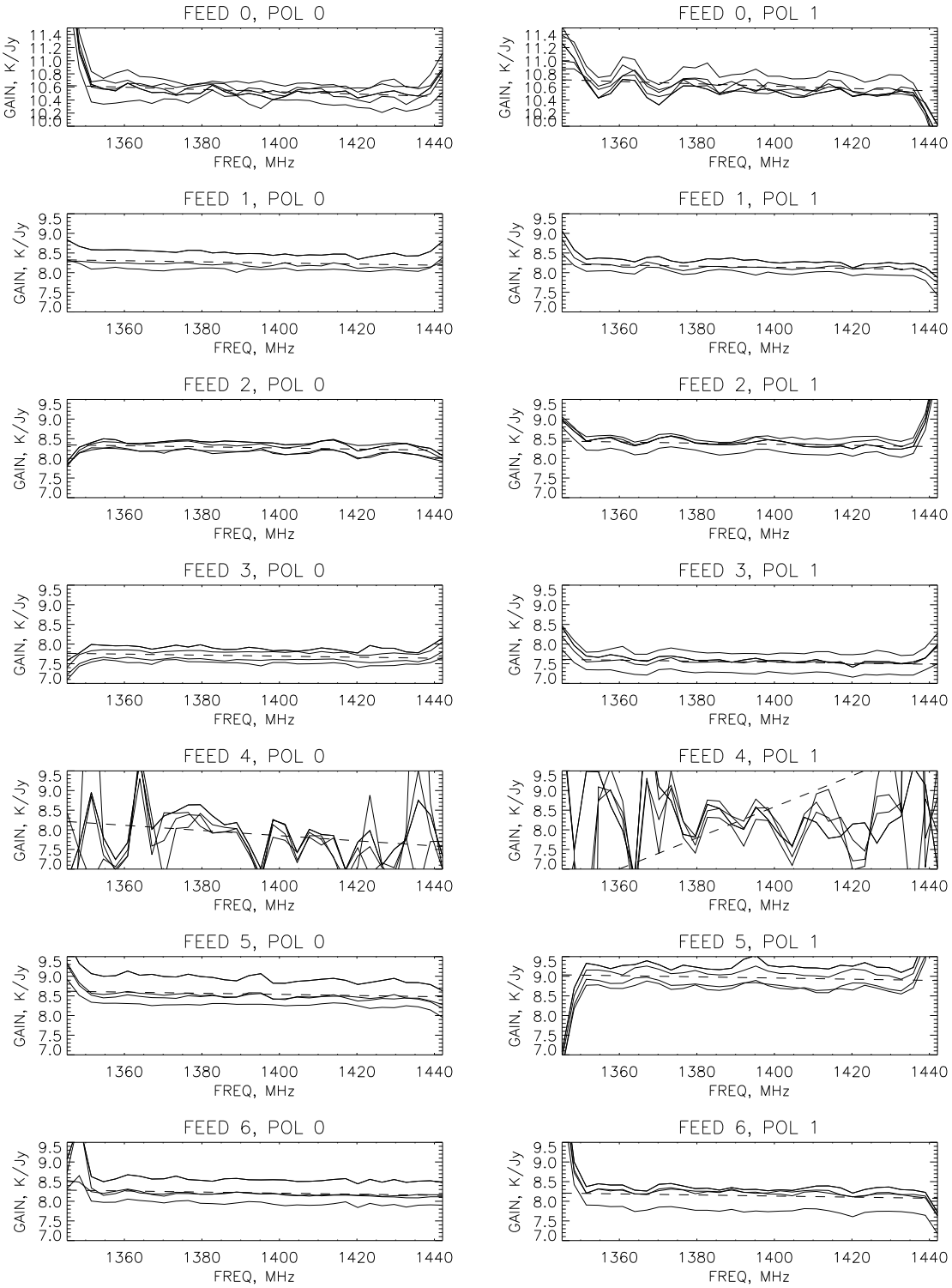

Fig. 4.— On-axis gain versus frequency for each feed/polarization entity derived from the cal values in Figure 2. Each solid line represents an independent observation and the dashed line is a fit to their average. Feed 4 values are no good.

8. TABLES OF FIDUCIAL VALUES AND SUMMARY

Here we provide tabular summaries of the fiducial values at 1420 MHz and also the frequency dependences. We don't discuss the system temperatures here; see §7.3.

8.1. Adopted Fiducial Values at 1420 MHz

Table 4 provides fiducial values for cal, gains, and efficiencies at 1420 MHz.

TABLE 4. ADOPTED FIDUCIAL VALUES

FEED	$T_{CAL,POL0}$ K	$T_{CAL,POL1}$ K	G_{max} K Jy^{-1}	η_{MB}	η_{FS}
0	10.8	10.1	10.7	0.69	0.11
1	9.8	10.6	8.3	0.56	0.19
2	11.2	10.2	8.5	0.55	0.20
3	10.6	9.6	7.8	0.50	0.19
4	10.1	10.4	8.3	0.59	0.18
5	9.6	10.1	8.7	0.58	0.19
6	10.4	10.3	8.3	0.56	0.17

8.2. Frequency Dependences

We fit the frequency dependence of the cals with a 7 degree polynomial defined as

$$T_{CAL} = \sum_{n=0}^{n=7} A_n (f - 1420)^n \ . \tag{20}$$

Table 5 gives the coefficients A_n for each feed/polarization, a digital copy of which is in the file `~heiles/gsr_carl/runspider/table5.ascii`. The IDL procedure `~heiles/gsr/spider/calget1.pro` evaluates the cal values and is valid for frequencies in the range 1344-1444 MHz.

The frequency dependence of all gains follows equation 18, a power law with slope -0.23.

We fit the frequency dependence of η_{MB} and η_{FS} with a linear function and obtained the following results. For the main beam,

$$\frac{1}{\eta_{MB}} \frac{d\eta_{MB}}{df} = +0.023 \ \ (100\text{MHz})^{-1} \tag{21a}$$

for all 7 beams. This change is tiny—the efficiencies change by just 2.3% of their value over 100 MHz—but systematic and statistically well-determined. The power-law equivalent is

$$\eta_{MB} \propto \left(\frac{f}{1420}\right)^{0.33} . \tag{21b}$$

The behavior of the first sidelobe is slightly more complicated. For beams 1-6 we have

$$\frac{1}{\eta_{FS}}\frac{d\eta_{FS}}{df} = +0.041 \quad (100\mathrm{MHz})^{-1} , \tag{21c}$$

whose power-law equivalent is

$$\eta_{FS} \propto \left(\frac{f}{1420}\right)^{0.58} . \tag{21d}$$

while for feed 0 there is no statistically significant frequency dependence.

Comparison of the power-law equivalents is interesting. The gains increase towards *lower* frequencies, while the beam efficiencies increase toward *higher* frequencies. For beams 1-6, at higher frequencies the first sidelobe increases relative to the main beam; this is probably a result of the aberrations being dependent on off-axis distance measured in wavelengths instead of centimeters. The increased main beam efficiency at higher frequency is probably caused by the increased spillover efficiency with frequency (equation 17); the power-law exponents are similar. And, of course, the gain is more affected by the size of the illuminated area on the primary by the spillover efficiency, so it increases towards lower frequency.

TABLE 5. POLYNOMIAL COEFFICIENTS FOR CAL VALUES

rcvr	pol	A0	A1	A2	A3	A4	A5	A6	A7
0	0	10.893	-3.14e-02	6.02e-04	1.69e-04	2.50e-06	-8.77e-08	-2.45e-09	-1.65e-11
0	1	10.277	-2.37e-02	1.81e-03	1.55e-04	-1.73e-06	-2.44e-07	-4.61e-09	-2.63e-11
1	0	9.872	-1.12e-02	1.75e-03	1.32e-04	-2.31e-07	-1.13e-07	-1.95e-09	-9.98e-12
1	1	10.582	-2.16e-02	1.58e-03	1.77e-04	-1.13e-06	-2.61e-07	-5.24e-09	-3.10e-11
2	0	11.069	1.89e-02	1.85e-04	2.59e-05	-1.17e-06	-7.56e-08	-1.11e-09	-4.96e-12
2	1	10.415	-5.78e-02	-1.08e-03	1.70e-04	9.41e-06	2.08e-07	2.23e-09	9.34e-12
3	0	10.650	3.09e-03	1.48e-04	8.31e-05	9.43e-07	-5.61e-08	-1.19e-09	-6.32e-12
3	1	9.545	-2.65e-02	6.87e-04	1.14e-04	1.27e-06	-6.03e-08	-1.39e-09	-8.10e-12
4	0	10.276	7.98e-02	-1.15e-03	-5.51e-04	-2.20e-05	-2.10e-07	2.08e-09	3.03e-11
4	1	10.943	1.67e-01	-2.96e-02	-2.37e-03	3.05e-05	5.11e-06	1.16e-07	7.98e-10
5	0	9.761	-2.81e-02	9.84e-04	1.36e-04	-1.86e-07	-1.57e-07	-3.03e-09	-1.69e-11
5	1	10.521	2.46e-02	-5.05e-03	-2.44e-05	1.19e-05	4.27e-07	5.78e-09	2.80e-11
6	0	10.537	-2.39e-02	5.76e-04	1.57e-04	7.96e-07	-1.57e-07	-3.40e-09	-2.01e-11
6	1	10.201	-8.58e-03	2.28e-03	1.48e-04	-2.82e-06	-2.89e-07	-5.49e-09	-3.26e-11

8.3. Three *ACTION ITEMS*

During our discussions above we encountered several issues that need further and continued attention. There exist many calibration data from ALFA commissioning and we encourage interested parties to address some of these issues using those data! We highlight these *ACTION ITEMS* here:

- In §6 we found that our two flux calibrator sources have "known" fluxes that differ by 9.3%. Clearly, this is unacceptable if we strive for accurate calibration.

  Our suggested *ACTION ITEM*: The direct measurements of on-axis gains should be refined by observing primary calibration sources whose fluxes are *truly* accurately known.

- In §4 we determined the relative cal values using the HI technique, and in §5 we determined the absolute cal values by comparing with the LDS HI survey. We noted that Giovanelli has found time variability in the cal values.

  Our suggested *ACTION ITEM*: use the HI technique on all areas mapped for HI to both maintain a historical record of changes and also gradually add to the precision with which the relative and absolute cal values are known at 1420 MHz.

- In §7.2 we found rapid variations of cal values with frequency and suggested that this might occur because of interference from either reflections or coupling between feeds, and speculated that these reflections would be sensitive to ALFA position angle and might changd with time.

  Our suggested *ACTION ITEM*: the dependences of cal values on frequency and ALFA rotation angle and time be determined and monitored regularly.

It is a pleasure to acknowledge my co-workers, Josh Goldston, Yvonne Kei-Nam Tang, Marko Krco, and Snezana Stanimirovic, who actually took the data. Special thanks go to Riccardo Giovanelli, who shared his calibration results, his discovery of time variation of the cal values, and was generally helpful and stimulating; and to Phil Perillat, who provided detailed information, essential software assistance, advice, and discussion; and to Snezana, who provided valuaable comments on an earlier version of this paper.

This work was supported in part by NSF grant 0406987.

REFERENCES

Cortés-Medellin, G. 2002, Arecibo Focal Array Memo Series, "Final Feed Selection Study for the Multi Beam Array System".

Deshpande, A. 2004, ALFA Memo of 2004 Nov 18.

Giovanelli, R., et al 2004, ALFA Memo 040920.

Hartmann, D. & Burton, W.B. 1997, Atlas of Galactic Neutral Hydrogen, Cambridge University Press.

Heiles, C. 2004, GALFA Tech Memo 2004-01.

Kalberla, P.M.W., Mebold, U., & Reif, K. 1982, A&A, 106, 109.

Rohlfs, K. & Wilson, T.L. 2000, Tools of Radio Astronomy, Springer-Verlag, chapters 5, 6.